ISSN 1062-8738, Bulletin of the Russian Academy of Sciences: Physics, 2022, Vol. 86, No. 7, pp. 846–851. © Allerton Press, Inc., 2022.
Russian Text © The Author(s), 2022, published in Izvestiya Rossiiskoi Akademii Nauk, Seriya Fizicheskaya, 2022, Vol. 86, No. 7, pp. 1019–1025.

Use of Phase Masks to Construct the Required Spatial Pattern of an Ultrasonic Field

D. A. Nikolaev[a, *], S. A. Petrosyan[a], S. A. Tsysar[a], P. B. Rosnitsky[a], and O. A. Sapozhnikov[a]

[a] *Faculty of Physics, Moscow State University, Moscow 119991 Russia*

**e-mail: da.nikolaev@physics.msu.ru*

Received February 14, 2022; revised February 28, 2022; accepted March 23, 2022

Abstract—A way of constructing a required distribution of an ultrasonic field in the range of megahertz frequencies in a liquid is developed by combining a system of two profiled solid plates (phase masks) positioned in front of a single-element piezoelectric emitter. The possibility of creating phase masks to control the spatial distribution of an acoustic field by changing the frequency of the radiation is studied.

DOI: 10.3103/S1062873822070231

INTRODUCTION

Controlling the spatiotemporal distribution of a wave field is required in many applications of acoustic waves [1–3]. Multi-element emitters can be used for this purpose, with each element operating independently of the others. In some problems, a large number of them may be required to create an acoustic field. Multi-element devices are difficult to make and control; in most cases, it is not possible to control the operating efficiency of each emitting channel in service [4]. Due to some technical limitations, actual devices now consist of 100–1000 elements, and even this quantity may not be enough to create a complex spatial field distribution. In addition, actual multichannel devices are not always available, due to their high cost.

Phase masks could be an alternative to multi-element emitters. Such masks are nonuniformly thick plates that allow the phase distribution of a transmitted wave to be altered selectively so we can obtain the required spatial distribution of a field [5]. This phase control is possible because of the difference in sound speeds in the environment and in the material of a plate.

Note that only the wave phase (hence the name) can be modulated using a single phase mask, while the amplitude of the wave changes weakly. To create the required spatial field distribution, we must control not only the phase but the amplitude of the acoustic field as well. The required spatial distribution of the amplitude and phase can be obtained using two spaced phase masks in the form of profiled plates [6], due to the phase modulation in each. Choosing the profile of plates and the distance between them allows us to select the conditions under which the plate closest to the emitter produces the required distribution of the amplitude of pressure on the surface of the second mask, which in turn creates the phase modulation needed to form the required spatial distribution of the amplitude and phase.

Phase masks can be made, for example, from photopolymer resin using 3D printing laser stereolithography with an accuracy of 0.1 mm.

In this work, we obtain an algorithm for calculating the thickness profile of two solid plates, the combination of which allows us to form a given distribution of the acoustic pressure in the transverse plane at a fixed distance from the emitter (Fig. 1a). We study the effect the nonuniform vibrational velocity of the emitter's surface on the quality of the field modulation by the set of two phase masks. An experimental model of two profiled plates is built on the basis of our results (Fig. 1b). We also consider the possibility of creating a multi-frequency phase mask that can be used to create given distributions of the pressure amplitude at several frequencies on a target plane.

CALCULATION OF PHASE MASKS

The phase delay of a transmitted wave is determined not only by the thickness, but also by the acoustic characteristics of the plate material and the immersion liquid (water). The sound speed and the density of water at an operating temperature of 22°C are 1491 m/s and 998 kg/m^3, respectively. Since a photopolymer resin was used in solving the considered problem, we preliminarily measured the acoustic parameters of the material. The speed of sound was determined by measuring the period of propagation of an ultrasonic pulse with a carrier frequency of 1 MHz through a plane-parallel sample of known thickness:

2509 ± 10 m/s. The measured density of the material was 1198 ± 1 kg/m^3.

Consider the problem in the following formulation. Using a plane emitter and phase masks, we need to create a distribution of intensity in the form of the letter "Π" on the target plane, which is parallel to the emitter surface and is located at some distance from it (Fig. 1a). The main limitation on the accuracy of the resulting spatial distribution of the acoustic field is the diffraction limit, so the characteristic scale of the nonuniformity of the predetermined field must exceed the wavelength in water. We used a two-stage approach (I, II) to calculate the system of masks. In stage (I) (the phase screen approximation, where the mask is considered to be infinitely thin and does not change the amplitude of a wave) an iterative procedure was used to calculate the required phase shifts in the planes of a mask. In stage (II), the field was calculated without the above approximation, and the required profile of the plates was determined. The iteration procedure at the first stage utilized the sequence of operations below.

(1) The real amplitude of pressure is determined according to a given intensity distribution in a plane located at distance Z_3 from the emitter (Fig. 1a). The phase of a wave is selected arbitrarily, for certainty we equate it to zero. For the system of a large wave size, it is sufficient to consider only propagating waves, so the distribution of the complex amplitude is defined at the nodes of a square grid with step $\Delta_{xy} = c_w/(2f)$, where f is the frequency and c_w is the speed of sound in water. The selected step is a half-wavelength in the medium and determines the resolution with which the phase mask is calculated.

(2) We use an angular spectrum [7] with a propagator of backward propagation from the plane Z_3 to Z_2 to calculate the complex amplitude of pressure.

(3) The field calculated at Z_2 is modified according to the phase screen approximation, but only with respect to the phase, which is randomly defined in interval $(-\pi, \pi)$ to start the iterative process at the next step.

(4) The next step is taken toward the emitter according to the modified field in the plane Z_2. We use the angular spectrum to calculate the complex amplitude of pressure in the plane Z_1 of the location of the first phase mask.

(5) The phase of the acoustic pressure is fixed on the plane Z_1, and the distribution of amplitude is replaced by the one along the emitter's surface that is valid for a mask in full contact with it. We use a piston model as a first approximation.

(6) An angular spectrum with a propagator of forward propagation is used to calculate the pressure from the plane Z_1 to the plane Z_2. The resulting phase distribution is used for the subsequent iterative process instead of the one initially defined at step 3.

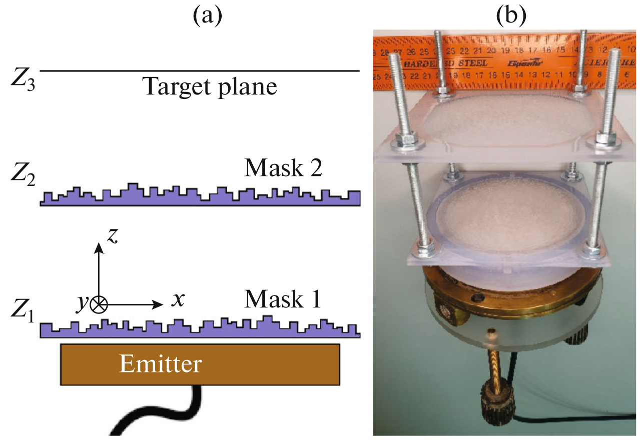

Fig. 1. (a) Geometry of the problem; (b) experimental model.

(7) Steps 4–6 are repeated until the sum of the point-to-point standard deviation of the amplitudes of pressure calculated on the plane Z_2 converges to the result obtained at step 2. The criterion for interrupting the iterative process is the difference stops decreasing with output to a constant. Around 1000 iterations were sufficient for the case considered in this work.

The required phase distributions beyond the plane Z_1 and in front of Z_2 are determined in this way. We recall that in front of Z_1 it is given by the field on the emitter's surface. Beyond Z_2, they are calculated according to the required field at step 2. The required phase delays $\Delta\varphi(x, y)$ for both masks are determined by the difference between the phases of the field at the input and output of each plane, allowing us to calculate the profile of each mask $z(x, y)$ at the grid nodes using the equation

$$z(x, y) = \frac{\Delta\varphi(x, y) - k_w Z_{max}}{k_m - k_w}, \quad (1)$$

where $k_w = \omega/c_w$, $k_m = \omega/c_m$ are the wavenumbers in water and the material of the mask, respectively, and Z_{max} is its maximum thickness.

At the second stage, the propagation of a wave from the emitter's surface to Z_2 through the first mask was modeled without using the phase screen approximation, taking into account its profile found after the first stage using Eq. (1). The field was calculated using the open source software package k-Wave MATLAB Toolbox [8], which uses a pseudo-spectral approach and allows us to model the propagation of an acoustic wave through a medium with a nonuniform sound speed, uneven absorption, and an inhomogeneous density. This procedure refined the required phase delay in the plane of the second mask and allowed determination of its thickness using Eq. (1). The same software was used later to calculate the propa-

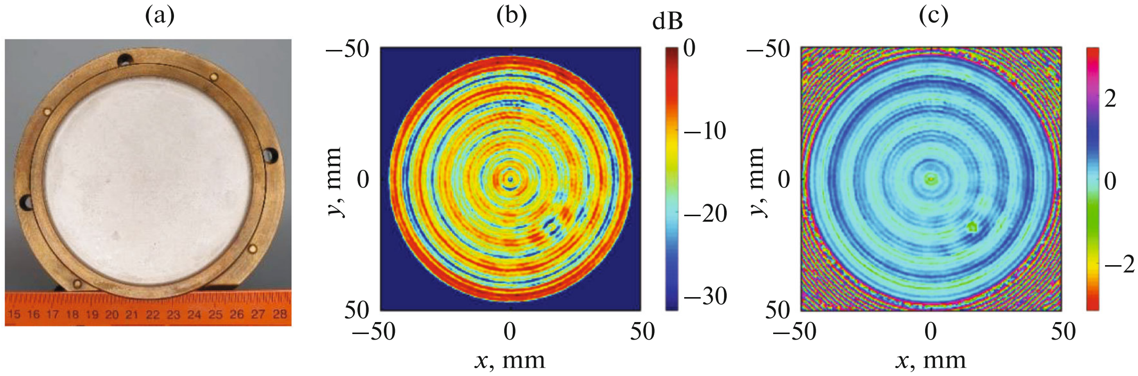

Fig. 2. (a) Piezoceramic emitter. (b) Normalized amplitude and (c) phase of the normal component of the vibrational velocity in water on the emitter's surface, determined via acoustic holography.

gation of a wave through the second mask to the target surface Z_3.

STUDYING THE EFFECT OF NONUNIFORM VIBRATIONS OF AN EMITTER

Phase masks are usually calculated using a piston approximation of the emitter's mode of operation [6, 9] that is not valid for actual transducers [10, 11].

The problem of determining the vibrational velocity of a surface can be solved via transient acoustic holography [12–14], which has developed rapidly in recent years. It allows us to calculate the spatial distributions of pressure and vibrational velocity, including on the surface of the emitter. To consider an actual spatial field distribution, we measured a hologram of a 93.5 mm-diameter transducer with a resonance frequency of 1.12 MHz (Fig. 2a) using a HGL-0200 capsule hydrophone with a sensing area diameter of 200 μm (Onda Corp., United States) that was moved by an UMS-3 micropositioning system (Precision Acoustics, United Kingdom). The obtained distributions of the amplitude and phase of the normal component of the vibrational velocity on the emitter's surface are shown in Figs. 2b, 2c, respectively.

It can be seen that the distributions of the amplitude and phase of the normal component of the vibrational velocity on the emitter's surface are strongly nonuniform. The concentric pattern is caused by the superposition of Lamb modes [11]. The rings with a higher velocity compared to the surrounding areas correspond to the places of the antinodes of standing waves, where radiation into water is most efficient.

To compare results obtained using the piston approximation and using the real distribution of the emitter's field, we calculated a set of masks to create a given distribution in the form of the letter "П" on the target plane Z_3 (Fig. 3a). Figure 3b shows the amplitude of pressure obtained on Z_3 using an approximation of the uniform vibration of the emitter. Figure 3c shows this distribution with allowance for its actual vibrational velocity. It is noticeable that in the second case (Fig. 3c), the calculated spatial pressure distribution at Z_3 is closer to the one given (Fig. 3a) with less pronounced speckles of radiation. Note also that the difference between these approaches is relatively small, and for certain applications it is possible to use the piston approximation when calculating acoustic masks.

Experimental verification was performed using printed phase masks (Fig. 1b) calculated taking into account the real vibrational velocity of the emitter's surface. The profiles of the first and second plates are shown in Figs. 3d, 3e, respectively. The units were printed using Accura 60 material on a Prox 800 SLA 3D printer. Figure 3f shows the profile of a surface of water under the action of acoustic radiation. The emitter and masks were adjusted parallel to the target plane, which coincided with the surface of the water. The relief bulges correspond to the high amplitude of the acoustic pressure.

MULTI-FREQUENCY MODULATION OF THE FIELD

The constructure of two phase plates made as described above allows changing an acoustic field in a given way only at one frequency, which limits their practical application. In this section, we propose a technique of multi-frequency modulation by dividing the phase mask into parts designed for different frequencies.

If the required distribution of pressure is sufficiently compact relative to the emitter's size but significantly exceeds the wavelength in the medium, the acoustic beam in the plane of the second mask (the one farther from the transducer) will also have a small transverse size after propagation. Therefore, for effec-

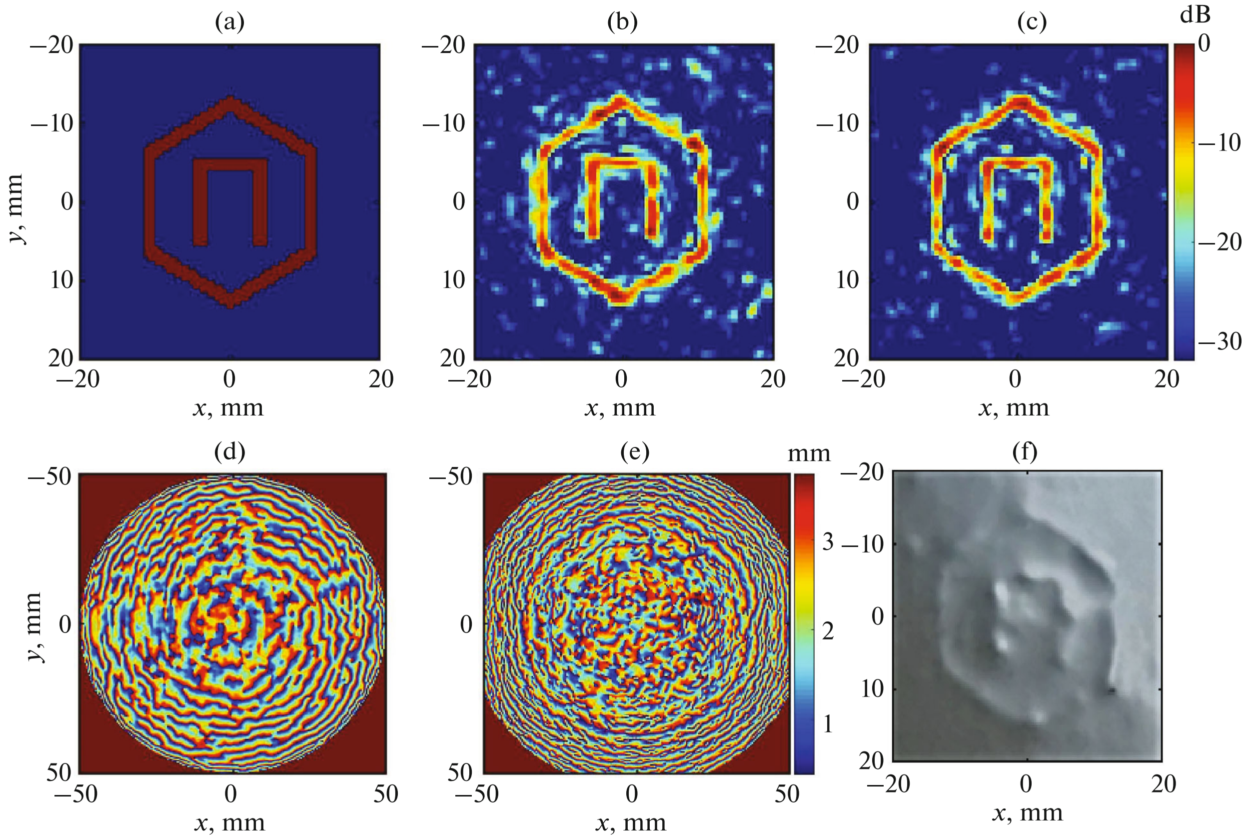

Fig. 3. (a) Distribution of the amplitude of pressure on a given target plane. The result of calculating (b) in the piston approximation of the emitter operation, (c) taking into account the measured hologram. The profile of the calculated masks at a distance of (d) Z_1 and (e) Z_2. (f) The relief of the water surface when the target plane and the water surface coincide.

tive modulation at several frequencies, acoustic beams should be directed from the target plane to different parts of the plane Z_2 (selecting the phase in step 1), which will form the required field distribution at the specified frequencies. It is convenient to choose the parts on both masks similar in shape and location. The corresponding part of the emitter under the first mask will then be used effectively to create a given distribution of pressure in the target plane. The procedure for selecting phase shifts and mask thickness for each frequency is similar to steps 3–7 of the algorithm described above.

The frequencies to which each mask part is tuned within the operating bandwidth of the emitter should be separated from one another enough so that the remaining parts perturb the acoustic field in the required distribution most uniformly. We must also consider that when the mask is divided into more parts, the energy of the acoustic field used for modulation at a particular frequency falls. The resulting distribution of pressure in the target plane therefore deviates more from the one specified.

To test the system operating in the multi-frequency mode, we first calculated field distributions φ and π (Figs. 4b, 4f) at 1.12 and 1.3 MHz, respectively. The acoustic mask was divided into two halves. The phase on the target plane (Figs. 4a, 4e) was chosen at step 1 so that the beam was maximally focused to the center of its mask part (Figs. 4c, 4g). The parts responsible for modulating at their own frequencies were combined after calculations. The propagation of a wave was then calculated through the combined mask, the result of which is shown in Figs. 4d, 4h.

Similarly, phase masks with four-frequency modulation in the range of 1–1.3 MHz with a step of 0.1 MHz were obtained. Four circles with a diameter of 1.5 mm were selected as the target distribution. Their centers were on the vertices of a square with sides of 4.5 mm. A quarter of the mask allowed focusing at the center of each circle. The calculated results show that the focal point of this system can be steered only by switching the frequency of the signal applied to the emitter (Figs. 4i–4l).

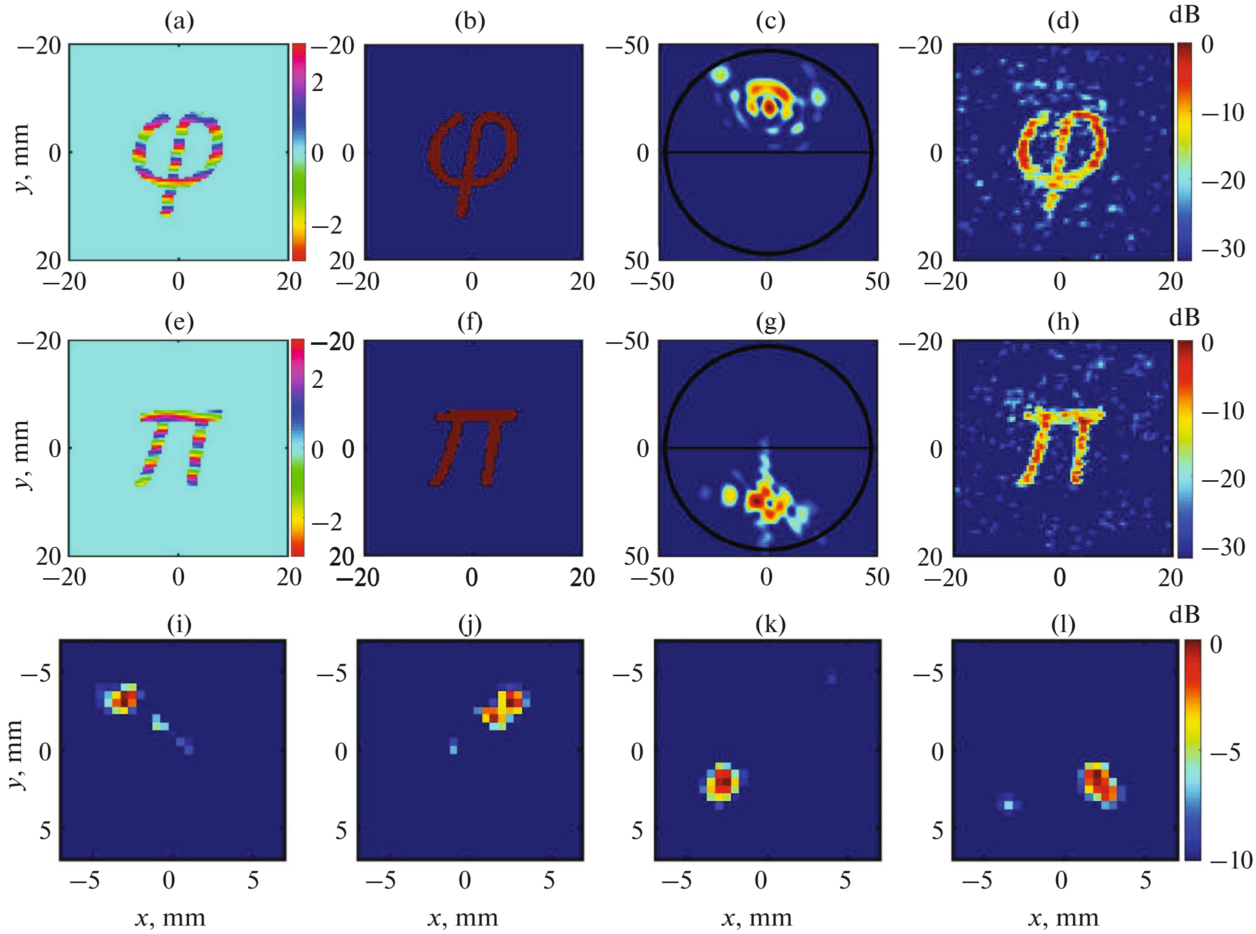

Fig. 4. Calculations for an acoustic wave with a frequency of 1.12MHz (first row) and 1.3 MHz (second row): (a, e) phase and (b, f) amplitude of the required distribution; (c, g) field at the surface of the second mask; (d, h) obtained distribution on the target plane. Four-frequency operation mode of the system for steering the focus at frequencies of (i) 1, (j) 1.1, (k), 1.2, and (l) 1.3 MHz (third row).

Improving the way of calculating phase masks can focus the field to a larger number of points. This system would therefore operate as a two-dimensional antenna array upon switching the frequency in a certain range, allowing us to scan a spatial region with no mechanical displacement of a single-element emitter.

CONCLUSIONS

We proposed a way of creating a required spatial field distribution in a plane using a system of two phase masks. It was shown that using the real vibrational velocity of the emitter's surface to calculate phase masks improves the quality of the target acoustic pressure distribution, which can be significant for some applications. It was demonstrated that the proposed approach allows controlling the spatial distribution of the field by changing the frequency of the signal.

FUNDING

This work was supported by the Moscow Polytechnical Museum; the Russian Foundation for Basic Research, project no. 19-32-90022; and Moscow State University's interdisciplinary research and educational school "Photonic and Quantum Technologies: Digital Medicine."

CONFLICT OF INTEREST

The authors declare that they have no conflicts of interest.

REFERENCES

1. Parfenov, V.A., Koudan, E.V., Krokhmal, A.A., et al., *Adv. Healthcare Mater.*, 2020, vol. 2020, 2000721.
2. Lee, J., Lee, C., and Shung, K.K., *IEEE Trans. Ultrason. Ferroelectr. Freq. Control*, 2010, vol. 57, no. 10, p. 2305.
3. Baresch, D. and Garbin, V., *Proc. Natl. Acad. Sci. U. S. A.*, 2020, vol. 117, no. 27, 15490.

4. Tsysar, S.A., Nikolaev, D.A., and Sapozhnikov, O.A., *Acoust. Phys.*, 2021, vol. 67, no. 3, p. 320.
5. Lalonde, R.J., Worthington, A., and Hunt, J.W., *IEEE Trans. Ultrason. Ferroelectr. Freq. Control*, 1993, vol. 40, no. 5, p. 592.
6. Brown, M.D., *Appl. Phys. Lett.*, 2019, vol. 115, 053701.
7. Nikolaev, D.A., Tsysar, S.A., and Sapozhnikov, O.A., *Bull. Russ. Acad. Sci.: Phys.*, 2021, vol. 85, no. 6, p. 658.
8. Treeby, B.E., Jaros, J., Rohrbach, D., et al., *Proc. 2014 IEEE Int. Ultrasonics Symposium*, Chicago, 2014, p. 146.
9. Zhang, J., Yang, Y., Zhu, B., et al., *Appl. Phys. Lett.*, 2018, vol. 113, 243502.
10. Canney, M.S., Bailey, M.R., Crum, L.A., et al., *J. Acoust. Soc. Am.*, 2008, vol. 124, no. 4, p. 2406.
11. Cathignol, D., Sapozhnikov, O.A., and Zhang, J., *J. Acoust. Soc. Am.*, 1997, vol. 101, no. 3, p. 1286.
12. Sapozhnikov, O.A., Tsysar, S.A., Khokhlova, V.A., et al., *J. Acoust. Soc. Am.*, 2015, vol. 138, no. 3, p. 1515.
13. Nikolaev, D.A., Tsysar, S.A., Khokhlova, V.A., et al., *J. Acoust. Soc. Am.*, 2021, vol. 149, no. 1, p. 386.
14. Petrosyan, S.A., Nikolaev, D.A., and Tsysar, S.A., *Bull. Russ. Acad. Sci.: Phys.*, 2021, vol. 85, no. 6, p. 647.

Translated by N. Podymova